A new three-band algorithm for estimating chlorophyll concentrations in turbid inland lakes

2010 Environ. Res. Lett. 5 044009

(http://iopscience.iop.org/1748-9326/5/4/044009)

Environ. Res. Lett. **5** (2010) 044009 (6pp) doi:10.1088/1748-9326/5/4/044009

A new three-band algorithm for estimating chlorophyll concentrations in turbid inland lakes

Hongtao Duan[1], Ronghua Ma[1,5], Yuanzhi Zhang[2], Steven Arthur Loiselle[3], Jingping Xu[4], Chenlu Zhao[1], Lin Zhou[1] and Linlin Shang[1]

[1] State Key Laboratory of Lake Science and Environment, Nanjing Institute of Geography and Limnology, Chinese Academy of Sciences, Nanjing, People's Republic of China
[2] Institute of Space and Earth Information Science, The Chinese University of Hong Kong, Hong Kong, People's Republic of China
[3] Dipartimento Farmaco Chimico Tecnologico, CSGI, University of Siena, Siena, Italy
[4] State Key Laboratory of Remote Sensing Science, Jointly Sponsored by the Institute of Remote Sensing Applications of Chinese Academy of Sciences and Beijing Normal University, Beijing, People's Republic of China

E-mail: mrhua2002@niglas.ac.cn

Received 25 July 2010
Accepted for publication 8 November 2010
Published 29 November 2010
Online at stacks.iop.org/ERL/5/044009

Abstract
A new three-band model was developed to estimate chlorophyll-a concentrations in turbid inland waters. This model makes a number of important improvements with respect to the three-band model commonly used, including lower restrictions on wavelength optimization and the use of coefficients which represent specific inherent optical properties. Results showed that the new model provides a significantly higher determination coefficient and lower root mean squared error (RMSE) with respect to the original model for upwelling data from Taihu Lake, China. The new model was tested using simulated data for the MERIS and GOCI satellite systems, showing high correlations with the former and poorer correlations with the latter, principally due to the lack of a 709 nm centered waveband. The new model provides numerous advantages, making it a suitable alternative for chlorophyll-a estimations in turbid and eutrophic waters.

Keywords: water color remote sensing, bio-optical model, absorption coefficient, inherent optical properties

1. Introduction

Chlorophyll-a is an important pigment in nearly all marine and freshwater algal species. The concentration of this pigment (Chla, mg m^{-3}) has often been used as a marker for phytoplankton biomass and in calculations of bio-production of many water bodies. The use of satellite based sensors to estimate Chla in large ecosystems provides numerous advantages with respect to standard field measurements (Kutser 2004). However, making such estimates in turbid lakes presents a number of difficulties, largely due to the complex optical conditions. In recent years, three-band reflectance models have been used with success in systems where Chla is not the dominant optical component (Dall'Olmo *et al* 2003, Gitelson *et al* 2008, Moses *et al* 2009, Xu *et al* 2009). These models are based on the following relationship between Chla and reflectance (R_{rs}):

$$[\text{Chla}] \propto [R_{rs}^{-1}(\lambda_1) - R_{rs}^{-1}(\lambda_2)]R_{rs}(\lambda_3) \quad (1)$$

where R_{rs} is a function of the inherent absorption ($a(\lambda)$) and scattering ($b_b(\lambda)$) properties of the medium, according to the

[5] Author to whom any correspondence should be addressed.

basic radiative transfer equation (Gordon *et al* 1988):

$$R_{rs} = \frac{ft}{Qn^2}\frac{b_b(\lambda)}{a(\lambda)+b_b(\lambda)}. \quad (2)$$

Absorption $a(\lambda)$ which can be separated into absorption related to phytoplankton biomass (a_{ph}), detritus (a_d), chromophoric dissolved organic matter (CDOM, a_g) and pure water (a_w), while $b_b(\lambda)$ is the measurement of total backscattering. The term f/Q, a function dependent on sun zenith angle (Morel and Gentili 1993), can be approximated to be 0.0945 (Gordon *et al* 1988), and $t/n^2 = 0.54$ (Clark 1981, Austin 1974).

In the three-band models developed to date, the difference between the reciprocal reflectance $R_{rs}^{-1}(\lambda_1)$ and $R_{rs}^{-1}(\lambda_2)$ (equation (1)) is approximated by

$$R_{rs}^{-1}(\lambda_1) - R_{rs}^{-1}(\lambda_2) \propto \frac{a_{ph}(\lambda_1) + a_w(\lambda_1) - a_w(\lambda_2)}{b_b} \quad (3)$$

based on the following assumptions: (a) b_b is spectrally invariant between λ_1 and λ_2; (b) $a_{ph}(\lambda_1) \gg a_{ph}(\lambda_2)$; (c) $a_d(\lambda_1) + a_g(\lambda_1) \approx a_d(\lambda_2) + a_g(\lambda_2)$. In lakes where high (non-phytoplankton-related) turbidity is present, such as Lake Taihu, assumptions (b) and (c) are not always valid. If these assumptions cannot be made, the difference between the reciprocal reflectances remains in its original form:

$$R_{rs}^{-1}(\lambda_1) - R_{rs}^{-1}(\lambda_2) \propto \{a_{ph}(\lambda_1) - a_{ph}(\lambda_2) + a_g(\lambda_1) - a_g(\lambda_2) + a_d(\lambda_1) - a_d(\lambda_2) + a_w(\lambda_1) - a_w(\lambda_2)\}\{b_b\}^{-1}. \quad (4)$$

In many turbid systems, a_g, a_d and a_w are independent of Chla, but are characteristic for the ecosystem. The sum of the wavelength differences $(a_g(\lambda_1) - a_g(\lambda_2) + a_d(\lambda_1) - a_d(\lambda_2) + a_w(\lambda 1) - a_w(\lambda_2))$ can then be treated as an ecosystem specific parameter c, making the equation

$$R_{rs}^{-1}(\lambda_1) - R_{rs}^{-1}(\lambda_2) \propto \frac{a_{ph}(\lambda_1) - a_{ph}(\lambda_2) + c}{b_b}. \quad (5)$$

In three-band models, the third spectral band, λ_3, is included to represent the effects of backscattering (b_b) with respect to absorption by water. In most cases, λ_3 is chosen to be in the near infrared (NIR) wavelengths, where reflectance by a_{ph}, a_d and a_g is minimal, i.e. $a(\lambda_3) \sim a_w$:

$$R_{rs}(\lambda_3) \propto \frac{b_b}{a_w(\lambda_3)}. \quad (6)$$

Based on equations (2), (5) and (6), the original relationship now becomes

$$[R_{rs}^{-1}(\lambda_1) - R_{rs}^{-1}(\lambda_2)] \cdot R_{rs}(\lambda_3) = \frac{a_{ph}(\lambda_1) - a_{ph}(\lambda_2) + c}{a_w(\lambda_3)}. \quad (7)$$

If the specific absorption of chlorophyll-a (a_{ph}^*, $m^{-1}(mg\ m^{-3})^{-1}$) is considered as $a_{ph} = a_{ph}^* \times [Chla]$ (Morel and Prieur 1977),

$$[Chla] = \frac{[R_{rs}^{-1}(\lambda_1) - R_{rs}^{-1}(\lambda_2)]R_{rs}(\lambda_3)a_w(\lambda_3) - c}{[a_{ph}^*(\lambda_1) - a_{ph}^*(\lambda_2)]}. \quad (8)$$

It should be noted that the difference in the specific absorption coefficients $[a_{ph}^*(\lambda_1) - a_{ph}^*(\lambda_2)]$ will not be constant throughout the ecosystem as the pigment composition will vary temporally and spatially. Equation (8) can be further simplified by combining the ecosystem specific optical properties into two variables, $\varepsilon = \frac{a_w(\lambda_3)}{[a_{ph}^*(\lambda_1) - a_{ph}^*(\lambda_2)]}$ and $\tau = \frac{c}{[a_{ph}^*(\lambda_1) - a_{ph}^*(\lambda_2)]}$:

$$[Chla] = \varepsilon[R_{rs}^{-1}(\lambda_1) - R_{rs}^{-1}(\lambda_2)]R_{rs}(\lambda_3) - \tau. \quad (9)$$

This new model contains two optically identifiable parameters that can be determined empirically by fitting of the measured Chla and observed reflectances. Most importantly, these parameters can be checked by comparing them with the inherent optical properties of the study waters. While the form of the equation is similar to the original three wavelength model, the proportionality constants are now associated with measurable quantities.

To compare models, we used measurements obtained in the field and simulated satellite based reflectance measurements for a large turbid lake in China. Lake Taihu (31.15 N, 120.15 E) presents a range of optical properties which are influenced by recurring phytoplankton blooms (Duan *et al* 2009b). MERIS is a medium spectral resolution, imaging spectrometer which has provided multispectral data for water color analysis since 2002 (Bezy *et al* 2000). GOCI (the Geostationary Ocean Color Imager) is the world's first geostationary ocean color multispectral system, with medium spatial resolution (500 m) and very high temporal resolution (refresh rate: 1 h). It is scheduled to be launched on 23 June 2010 by the Republic of Korea (ROK), and will include Lake Taihu in its coverage area.

In the present study, we compare the performance of the new three-band model to standard Chla models using measured spectral reflectances and *in situ* measurements. We examine the physical significance of the parameters used in the new three-band model. Finally, we assess the potential use of this model to estimate Chla using MERIS and GOCI reflectance data.

2. Methods

2.1. Data

Four data collection campaigns were performed in October 2004, June 2007, October 2008 and April–May 2010 in Lake Taihu, China (table 1). At each station GPS coordinates (0.3–3 m accuracy) were recorded and water samples were collected from the surface to a depth of 30 cm for measurement in the laboratory. Remote sensing reflectance was measured with a FieldSpec Pro Dual VNIR (ASD, USA) using NASA protocols (Mueller *et al* 2003). The absorption by total suspended matter, pigment, detritus and CDOM were determined using the quantitative filter technique with a Shimadzu UV2401 spectrophotometer (Shimadzu, Tokyo, Japan). Chla concentrations were extracted using 90% ethanol and measured with a UV2401 spectrophotometer. The concentrations of total suspended solids (TSM) were determined gravimetrically.

Table 1. Descriptive statistics of the optical water quality parameters measured in Lake Taihu: Chla, chlorophyll-a; TSS, total suspended solids; $a_g(440)$, absorption coefficient of CDOM at 440 nm; $a_d(440)$, absorption coefficient of detritus at 440 nm; $a_{ph}(440)$, absorption coefficient of phytoplankton at 440 nm; $a_{ph}(675)$, absorption coefficient of phytoplankton at 675 nm. (Note: n represents the number of sampling points each year; AVE means the average value, MAX means the maximum value and MIN means the minimum value.)

	2004 ($n = 45$)			2007 ($n = 35$)			2008 ($n = 83$)			2010 ($n = 80$)		
	AVE	MAX	MIN	AVE	MAX	MIN	AVE	MAX	MIN	AVE	MAX	MIN
Chla (μg l^{-1})	13.12	22.54	4.98	12.39	55.24	2.37	22.35	108.90	3.35	8.94	46.98	0.13
TSS (mg l^{-1})	60.14	169.47	13.08	34.23	107.00	10.32	35.58	90.45	7.80	41.37	162.73	9.90
$a_g(440)$ (m^{-1})	1.14	2.01	0.45	1.20	2.27	0.45	0.91	1.67	0.40	0.63	1.34	0.29
$a_d(440)$ (m^{-1})	2.91	6.77	0.64	1.43	3.18	0.59	2.12	5.66	0.60	1.86	7.77	0.53
$a_{ph}(440)$ (m^{-1})	1.07	2.90	0.44	0.74	1.43	0.87	0.42	1.86	0.11	1.20	7.81	0.21
$a_{ph}(675)$ (m^{-1})	0.30	0.52	0.13	0.27	0.23	0.10	0.22	1.09	0.06	0.57	4.13	0.07

Table 2. The new three-band model compared with original three-band model.

	Original three-band model					New three-band model						
Datasets	λ_1	λ_2	λ_3	R^2	RMSE	λ_1	λ_2	λ_3	R^2	RMSE	ε	τ
2004	671	710	714	0.50	2.77	665	689	814	0.59	2.52	294.71	11.61
2007	674	711	822	0.86	4.98	662	672	900	0.93	3.55	−1153.91	−3.76
2008	685	710	862	0.88	5.81	688	705	862	0.89	5.76	649.26	25.22
2010	678	710	854	0.89	3.58	690	694	853	0.90	3.48	928.42	6.64
All	686	710	839	0.66	8.25	688	692	870	0.78	6.64	1495.85	7.18

2.2. Fitting method

In order to optimize the three band positions of equation (9), an iterative fitting algorithm with linear least squares was developed using MATLAB software. The algorithm minimizes the sum of squared residuals between the measured concentration and the value provided by a model. The root mean squared error (RMSE) is employed to assess the performance of the model as

$$\mathrm{RMSE} = \sqrt{\frac{\sum_{i=1}^{n} (\mathrm{Chla}_{\mathrm{mea},i} - \mathrm{Chla}_{\mathrm{pre},i})^2}{n}} \qquad (10)$$

where n is the number of samples and $\mathrm{Chla}_{\mathrm{mea},i}$ and $\mathrm{Chla}_{\mathrm{pre},i}$ are the measured and predicted Chla values.

3. Results and discussion

3.1. Model comparison

Table 2 shows the results of both models in estimating Chla during the four measurement campaigns in Lake Taihu based on field reflectance measurements. In all campaigns, the new three-band model provided a higher determination coefficient (R^2) and a smaller RMSE than the original model. Considering the whole dataset, the new model predicted Chla with a R^2 of 0.78 with respect to 0.66 for the original model. For Chla ranging from 0.13 to 108.90 μg l^{-1}, the RMSE for the new model did not exceed 6.64 μg l^{-1}. In the light of these results, the new model provided better results than the older model.

Another restriction with the original three-band model is related to the limits of the wavelength intervals for each spectral band λ_1, λ_2 and λ_3 with respect to the following assumptions: (1) λ_1 should be located at the maximum phytoplankton absorption; (2) the absorption by detritus and CDOM at λ_2 should be similar to that at λ_1, while $a_{ph}(\lambda_2) \ll a_{ph}(\lambda_1)$; (3) reflectance at λ_3 should be least affected by differences in absorption while remaining sensitive to the variability in scattering and (4) the total backscattering coefficients for λ_1, λ_2 and λ_3, are approximately equal. To meet the above requirements, each wavelength is restricted within certain intervals (Gitelson *et al* 2009). By using the spectral reflectance measured over Lake Taihu in the 2004–2010 dataset, it is possible to identify these wavelength limits (figure 1).

In the visible and NIR spectral regions, reflectance was highly variable and similar to typical reflectance spectra collected in turbid waters (Gitelson *et al* 2006). Absorption by dissolved organic matter and detritus as well as backscattering by particulate matter combines to determine the spectral distribution of reflectance. The reflectance in the 400–500 nm interval was relatively low with respect to that between 500 and 600 nm. Reflectance above 600 nm presented several spectral features: (a) a slight reflectance reduction around 620 nm probably linked to phycocyanin absorption from cyanobacteria (Simis *et al* 2005); (b) a minimum reflectance around 675 nm likely to be related to chlorophyll-a absorption, although no direct correlation between Chla and R_{675} was observed. The peak between 670 and 715 nm observed in most reflectance curves can be associated with high backscattering and minimum absorption by all optically active constituents in this wavelength interval (Gitelson *et al* 2008). The optimal wavelengths which meet the four assumptions of the original three-band model fall into the following intervals: 650–690 nm for λ_1, 710–740 nm for λ_2, and >750 nm for λ_3.

The optimal positions for each wavelength of the three-band model will depend on the optical properties of the study waters. For example, in Chesapeake Bay, the optimal λ_1, λ_2, and λ_3 were found in the intervals between 674–676, 691–698, and 723–739 nm, respectively (Gitelson *et al* 2007); in

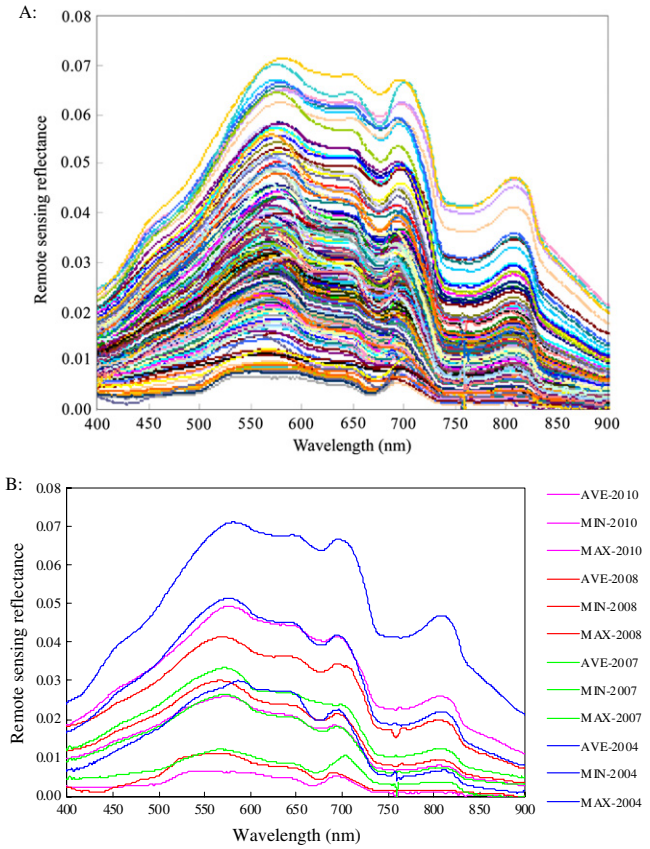

Figure 1. Reflectance spectra measured over Lake Taihu, China: (A) all data during 2004–2010; (B) the maximum, minimum and average data of each year.

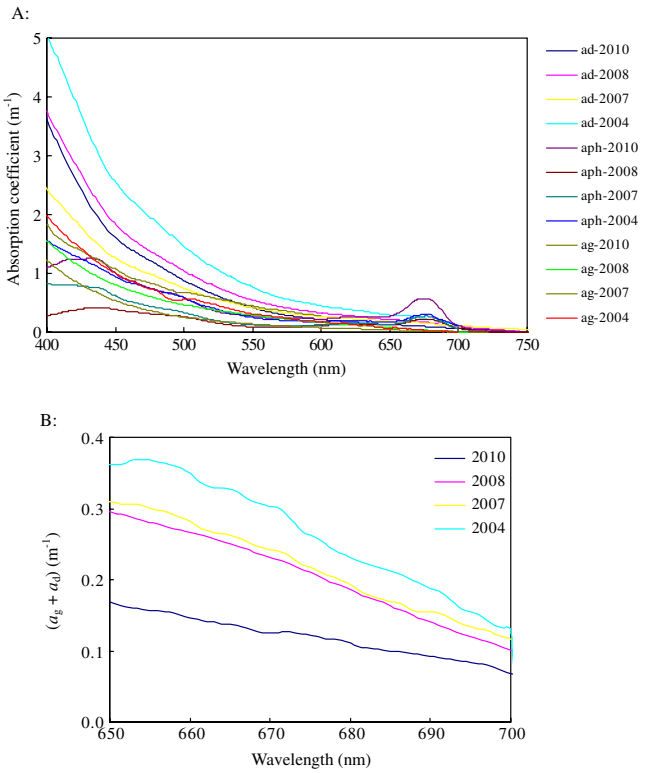

Figure 2. (A) Average spectral absorption of detritus (a_d), phytoplankton (a_{ph}) and CDOM (a_g) for each year during 2004–2010; (B) the sum of the average spectral absorption of detritus (a_d) and CDOM (a_g) between 650 and 700 nm.

Shitoukoumen Reservoir and Songhua Lake, these intervals were 650–680 nm, 670–700 nm, and >700 nm (Xu *et al* 2009); in lakes and reservoirs of Nebraska and Iowa, they were 658–674 nm, 700–735 nm, and 733–780 nm (Gitelson *et al* 2008); in Lake Taihu, they were 660–690, 700–750, and 730–750 nm (Zhang *et al* 2009); in Lake Chagan, they were 670–710 nm, 660–690 nm, and 710–750 nm (Duan *et al* 2009a). Therefore, the selection of wavelength intervals for each band depends on *a priori* knowledge of the optical conditions of the study waters. It is important to note that the selection of wavelength intervals will influence the Chla estimation. For example, using the 2007 Lake Taihu dataset, if different wavelength ranges for λ_1, λ_2, and λ_3 are compared, in one case 650–685 nm, 690–730 nm, and 730–780 nm, in the other 650–690 nm, 710–740 nm, and 750–900 nm, the determination coefficient between estimated and measured Chla will vary from 0.82 to 0.86, respectively.

In many eutrophic and turbid lakes, the dominance of absorption related to phytoplankton pigments with respect to detritus and CDOM may not occur, negating the second assumption of the original model (figure 2(A)). Furthermore, in such optical conditions, the difference between $[a_d(\lambda_1) + a_g(\lambda_1)]$ and $[a_d(\lambda_2) + a_g(\lambda_2)]$ may not be zero (figure 2(B)). Finally, $a_{ph}(\lambda_1)$ may not always be far larger than $a_{ph}(\lambda_2)$, especially when λ_1 is located beyond the peak near 680 nm (figure 2(A)), going against the first assumption. The new three-band model, by including c, does not require such rigid assumptions. It has the further advantage that it does not depend on specific wavelength ranges in the estimation of the three optimal wavelengths.

The new model makes fewer rigid assumptions due to the fact that the specific optical properties of the lake are included in the calibration equation. As a results, larger wavelength intervals are possible, $\lambda_1 > 600$ nm, $\lambda_2 > 600$ nm, $\lambda_3 > 750$ nm. This allows for a less subjective selection of wavelengths as well as allowing for better inter-lake comparison.

3.2. Applying the new model to MERIS and GOCI

MERIS was designed mainly for ocean and coastal water remote sensing and therefore has a large number of wavebands specifically selected for ocean color. GOCI provides a very high temporal resolution with a smaller number of wavebands. We investigated the potential use of the new three-band model for both of these remote imagining spectrometers using simulated reflectance data. Field spectra were resampled with respect to their center wavelengths for the MERIS spectral bands (413, 443, 490, 510, 560, 620, 665, 681, 709, 754, 761, 779, 865, 886, 900 nm) and GOCI spectral bands (412, 443, 490, 555, 660, 680, 745, 865 nm). To meet the requirements of the new model, nine bands from 665 to 900 nm were used for MERIS, but only four bands (660, 680, 745, 865 nm)

Table 3. Results of the new three-band model applied to MERIS and GOCI in Lake Taihu.

	MERIS							GOCI						
Datasets	λ_1	λ_2	λ_3	R^2	RMSE	ε	τ	λ_1	λ_2	λ_3	R^2	RMSE	ε	τ
2004	665	709	754	0.44	2.94	105.17	15.82	680	745	865	0.12	3.67	30.50	21.99
2007	681	709	754	0.85	5.20	146.35	14.20	680	745	865	0.30	11.07	83.55	40.66
2008	681	709	865	0.87	6.06	404.24	24.84	680	745	865	0.73	8.83	246.63	101.30
2010	681	709	754	0.89	3.67	82.52	9.56	660	745	865	0.59	7.07	89.67	37.47
All	681	709	865	0.62	8.75	237.75	16.13	680	745	865	0.35	11.41	116.04	51.18

Table 4. The new three-band model applied to MERIS while λ_1 at 665 nm, λ_2 at 709 nm, and λ_3 at 754 nm.

Datasets	R^2	RMSE	ε	τ
2004	0.44	2.94	105.17	15.82
2007	0.82	5.66	145.39	16.91
2008	0.83	7.10	245.96	29.62
2010	0.87	3.91	54.91	8.78
All	0.39	10.94	74.64	16.15

were used for GOCI. The results show that the new three-band model successfully estimates Chla using the MERIS spectral bands with high determination coefficients and low RMSEs. For most datasets, the optimal wavebands selected were 681 nm (λ_1), 709 nm (λ_2) and 754 nm (λ_3) (table 3). Two datasets showed the best results for 865 nm (λ_3), but NIR bands beyond 750 nm are rarely used for aircraft and satellite based remote sensing of water (Moses *et al* 2009). Likewise, the 681 nm band is strongly affected by variation in phytoplankton fluorescence, leading sometimes to difficulties for remote observations. To examine the use of the model for more commonly used wavebands (λ_1 at 665 nm, λ_2 at 709 nm, and λ_3 at 753 nm) a new analysis was made, showing slightly lower determination coefficients (table 4). By comparison, the highest determination coefficients were found for the hyperspectral data, followed by the optimal wavebands and finally by the most common MERIS wavebands (tables 2–4). The GOCI simulated reflectance data provided poorer estimates with respect to the MERIS sensors, even though the results from 2008 to 2010 gave an elevated determination coefficient (table 3). The loss in precision for the GOCI estimates can be associated with the lack of a reflectance waveband at 709 nm (λ_2).

3.3. Physical significance of ε and τ

The parameters c, ε, and τ in the new model are directly linked to specific inherent optical properties of the study waters, as ε represents $\frac{a_w(\lambda_3)}{[a^*_{ph}(\lambda_1)-a^*_{ph}(\lambda_2)]}$, τ represents $\frac{c}{[a^*_{ph}(\lambda_1)-a^*_{ph}(\lambda_2)]}$, and c is the sum of $(a_g(\lambda_1) - a_g(\lambda_2) + a_d(\lambda_1) - a_d(\lambda_2) + a_w(\lambda_1) - a_w(\lambda_2))$. The comparison between ε estimated from reflectance data with respect to ε determined from the inherent optical properties of Lake Taihu during different measurement campaigns shows a high 1:1 correlation (figure 3(A)). A negative correlation ($r = -0.93$) for τ (figure 3(B)) occurs. This is largely due to the lack of *in situ* absorption data (a_g and a_d) at wavelengths greater than 700 nm, where zero absorption was assumed. As expected, these parameters showed a wide interannual variation (tables 2 and 3).

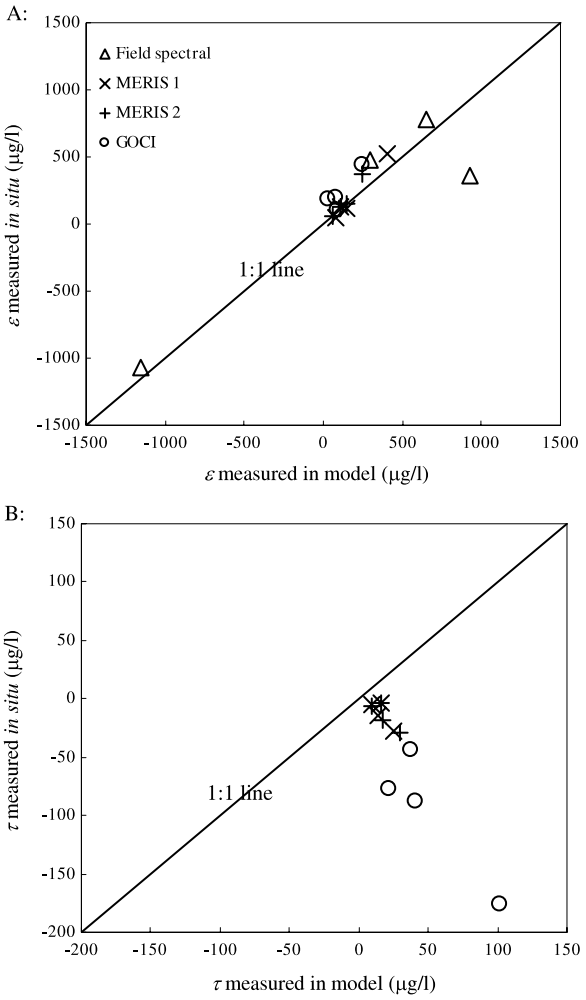

Figure 3. Scatter plot of the parameters estimated using the new three-band model against measured *in situ* data: (A) ε; (B) τ. In this study, a_w come from (Smith and Baker 1981); a_{ph}, a_d and a_g measured *in situ* come from average data of each year during 2004–2010; 'Field spectral' represents the new three-band model dataset of table 2; 'MERIS 1' represents the MERIS dataset of table 3; 'MERIS 2' represents the dataset of table 4; 'GOCI' represents the GOCI dataset of table 3.

The original three-band model is parameterized using a linear regression between $[R_{rs}^{-1}(\lambda_1) - R_{rs}^{-1}(\lambda_2)]R_{rs}(\lambda_3)$ and Chla concentrations, where the slope and intercept are not intended to be related to specific optical properties and provide no information to compare optically different

waters. Furthermore, the model assumes that the Chla specific absorption coefficient, a^*_{ph}, remains constant, whereas this coefficient will vary in relation to differences in the phytoplankton community and physiological state. In the new three-band model, a^*_{ph} is not considered constant and is included in the parameters ε and τ, the latter also including the errors in the absorption coefficients of the major optical constituents of the water body. Making fewer assumptions and linking model parameters to the optical conditions of the water body, the new model responds better to the complex conditions of turbid and eutrophic waters.

4. Summary

In the present study, a new three-band model was developed to estimate Chla in eutrophic and turbid waters. Unlike the original three-band model, larger waveband intervals can be used ($\lambda_1 > 600$ nm, $\lambda_2 > 600$ nm, $\lambda_3 > 750$ nm). Furthermore, the parameters that result from the fitting procedure, ε and τ, have clear links to the inherent optical properties of the water body. The new model was shown to provide a higher precision than the original three-wavelength model for the turbid and eutrophic waters of Lake Taihu. Importantly, it can be used with MERIS data, while its use with the new GOCI data is reduced due to the lack of a waveband at 709 nm. Since the dataset has a broad range of water component concentrations and shows a seasonal and interannual variability, it is very representative for Lake Taihu and other lake ecosystems. The three-wavelength model presented here offers a robust alternative to other Chla estimation approaches currently being used and can be used widely.

Acknowledgments

We would like to acknowledge the financial support provided by the Knowledge Innovation Program of the Chinese Academy of Sciences (No. KZCX2-EW-QN308 and No. KZCX2-YW-QN311) and the National Natural Science Foundation of China (No. 40801137 and No. 40871168).

References

Austin R W 1974 *Inherent Spectral Radiance Signatures of the Ocean Surface: in Ocean Color Analysis* 7410 (San Diego, CA: Scripps Institute of Oceanography)

Bezy J L, Delwart S and Rast M 2000 MERIS—a new generation of ocean-colour sensor onboard Envisat *ESA Bull-Eur. Space* **103** 48–56

Clark D K 1981 *Phytoplankton Algorithm for the Nimbus-7 CZCS (Coastal Zone Color Scanner), in Oceanography From Space* ed J R F Gower (New York: Plenum)

Dall'Olmo G, Gitelson A A and Rundquist D C 2003 Towards a unified approach for remote estimation of chlorophyll-a in both terrestrial vegetation and turbid productive waters *Geophys. Res. Lett.* **30** 1938

Duan H, Ma R, Xu J, Zhang Y and Zhang B 2009a Comparison of different semi-empirical algorithms to estimate chlorophyll-a concentration in inland lake water *Environ. Monit. Assess.* **170** 231–44

Duan H, Ma R, Xu X, Kong F, Zhang S, Kong W, Hao J and Shang L 2009b Two-decade reconstruction of algal blooms in China's Lake Taihu *Environ. Sci. Technol.* **43** 3522–8

Gitelson A A, Dall'Olmo G, Moses W, Rundquist D C, Barrow T, Fisher T R, Gurlin D and Holz J 2008 A simple semi-analytical model for remote estimation of chlorophyll-a in turbid waters: validation *Remote Sens. Environ.* **112** 3582–93

Gitelson A A, Gurlin D, Moses W J and Barrow T 2009 A bio-optical algorithm for the remote estimation of the chlorophyll-a concentration in case 2 waters *Environ. Res. Lett.* **4** 045003

Gitelson A A, Keydan G P and Merzlyak M N 2006 Three-band model for noninvasive estimation of chlorophyll, carotenoids, and anthocyanin contents in higher plant leaves *Geophys. Res. Lett.* **33** L11402

Gitelson A A, Schalles J F and Hladik C M 2007 Remote chlorophyll-a retrieval in turbid, productive estuaries: Chesapeake Bay case study *Remote Sens. Environ.* **109** 464–72

Gordon H R, Brown O B, Evans R H, Brown J W, Smith R C, Baker K S and Clark D K 1988 A semianalytic radiance model of ocean color *J. Geophys. Res.-Atmos.* **93** 10909–24

Kutser T 2004 Quantitative detection of chlorophyll in cyanobacterial blooms by satellite remote sensing *Limnol. Oceanogr.* **49** 2179–89

Morel A and Gentili B 1993 Diffuse-reflectance of oceanic waters. 2. Bidirectional aspects *Appl. Opt.* **32** 6864–79

Morel A and Prieur L 1977 Analysis of variations in ocean color *Limnol. Oceanogr.* **22** 709–22

Moses W J, Gitelson A A, Berdnikov S and Povazhnyy V 2009 Satellite estimation of chlorophyll-a concentration using the red and NIR bands of MERIS—the Azov sea case study *IEEE Trans. Geosci. Remote Sens.* **6** 845–9

Mueller J L, Fargion G S and Mcclain C R 2003 *Ocean Optics Protocols for Satellite Ocean Color Sensor Validation* (Maryland: Greenbelt) Revision 4

Simis S G H, Peters S W M and Gons H J 2005 Remote sensing of the cyanobacterial pigment phycocyanin in turbid inland water *Limnol. Oceanogr.* **50** 237–45

Smith R C and Baker K S 1981 Optical-properties of the clearest natural-waters (200–800 nm) *Appl. Opt.* **20** 177–84

Xu J P, Li F, Zhang B, Song K S, Wang Z M, Liu D W and Zhang G X 2009 Estimation of chlorophyll-a concentration using field spectral data: a case study in inland Case-II waters, North China *Environ. Monit. Assess.* **158** 105–16

Zhang Y L, Liu M L, Qin B Q, van der Woerd H J, Li J S and Li Y L 2009 Modeling remote-sensing reflectance and retrieving chlorphyll-a concentration in extremely Turbid case-2 waters (Lake Taihu, China) *IEEE Trans. Geosci. Remote Sens.* **47** 1937–48